Investigation of Microstructure and Tribological Properties of Al/Al_2O_3+Gr Hybrid Composite

M. A. MATARA[a], I. CSÁKI[a*], G. POPESCU[a], M. LUCACI[b], M. LUNGU[b]
[a]*University "Politehnica" Bucharest, Materials Science and Engineering Department, Splaiul Independentei Blvd. no. 313, 060042, Bucharest, Romania*
[b]*INCDIE ICPE-CA, Bucharest, Romania*

The present work aim is the investigation on the microstructure and tribological properties behavior of a hybrid aluminum matrix composites reinforced with 4.5 wt.% alumina (Al_2O_3) and 0.5 wt.% graphite (Gr) particles. Alumina particles were used as reinforcing material because it provides a high strength and hardness and graphite particles for its lubricating properties. The composite material was processed by powder metallurgy route. The powders mixture having the above mentioned composition was mixed using a high energy planetary ball mill for 3 h at 250 rpm. Starting from non-granulated and granulated powders mixtures, green compacts were obtained by compacting with pressures ranging between 100 and 600 MPa using a uniaxial hydraulic press, followed by a three steps sintering process realized at 300^0C for 30 min, 450^0C for 30 min and at 620^0C for 1 h in argon atmosphere. Tribological properties were investigated due to their importance that derives from the fact that the friction phenomenon particularly affects machinery and equipment functionality. The results were influenced by the processing of the powders mixtures, the compacting pressure applied to obtain green compacts, the homogeneity of the obtained microstructure after sintering process and the tribological testing conditions.

(Received April 4, 2015; accepted October 28, 2015)

Keywords: Hybrid composites, Compacting, Sintering, Tribology

1. Introduction

In the last decades, aluminum matrix composites (AMCs) are increasingly used as substitutes for monolithic materials due to their superior properties such as low density, greater strength, high stiffness, controlled thermal expansion coefficient, improved high temperature properties, improved abrasion and wear resistance [1]. There are three methods used to obtain AMCs: liquid-state process (stir casting, pressure infiltration), semi-solid state process (compocasting) and solid-state process (mechanical alloying, powder metallurgy) [2, 3]. The last method is more and more used due to the possibility of a homogenous dispersion of the reinforcing particles in the metal matrix avoiding particle clusters formation [2]. In the last years there is an increasing interest in Hybrid Metal Matrix Composites (HMM(C) which can be used for different applications which require combined strength, high wear resistance, and high thermal conductivity. HMMCs have 2 or more reinforcements, improving the material properties [3, 4]. The most commonly used reinforcements for HMMCs are SiC, Al_2O_3 and Gr. Due to the properties enhancement provided by these ceramic particles, the HMMCs find applications in automotive as cylinder blocks, pistons, callipers and brake disks. Al_2O_3 used as reinforcement for MMCs provides high strength, hardness and increases the wear resistance while having low density. In order to use these composites in automotive applications, they need to have good sliding properties [5]. The most widely used solid lubricant is Graphite (Gr) due to its self-lubrication properties [5-9]. R. Deaquino-Lara et al. reported an improvement on strength, hardness and dry wear resistance using graphite as reinforcement in Al metal matrix. [10]. P. Ravindran et al. investigated the tribological properties of powder metallurgy processed hybrid composites with the addition of graphite as solid lubricant and resulted that the composites with 5 wt.% Gr showed excellent wear resistance and friction coefficients. The addition of Gr particles as the second reinforcement in the Al matrix improves friction and wear properties [11,12].

A. Baradeswaran studied the mechanical and wear properties of $7075/Al_2O_3$/graphite hybrid composites [11].

In this paper tribological properties and microstructure of an Al/Al_2O_3/Gr hybrid composite containing 95.2 wt.% Al, 4.3 wt.% Al_2O_3 and 0.5 wt.% Gr were studied by varying the processing parameters of the composite that was obtained by powder metallurgy route starting from non-granulated (NGP) and granulated pure powders (GP). Al_2O_3 was used as a reinforcing material due to its refractory and high hardness characteristics and Gr provides a low coefficient of friction and low wear due to its hexagonal structure.

2. Experimental details

Materials used in this study were high purity Al as metal matrix and Al_2O_3 and Gr as reinforcements. The Al/Al_2O_3/Gr composites containing 95.2 wt.% Al, 4.3 wt.% Al_2O_3 and 0.5 wt.% Gr were processed by powder

metallurgy route (mechanical alloying, compacting and sintering).

The powders mixtures were mechanical alloyed in a RETSCH PM 400 planetary ball mill for 3 h at 250 rpm with a steel balls to powder ratio of 10:1 and 1 wt.% zinc stearate as process control agent in order to avoid powders agglomeration and to prevent powders deposition on the vial walls and on the steel balls.

By axial pressing between 100 and 600 MPa some green compacts in cylindrical shape having 17 mm in diameter and 3.5±0.5 in height were obtained from non-granulated and granulated powders mixtures.

The granulation of the powders mixtures was performed after their compaction with a pressure of 100 MPa, crushing and sieving between 125 and 315 μm in order to increase the powders ability to flow. After that all the green compacts were subjected to a three steps sintering process realized at 300^0C for 30 min, 450^0C for 30 min and at 620^0C for 1 h in argon atmosphere. The sintered specimens made of non-granulated powders mixtures (NGPM-SS) and the sintered ones made of granulated powders mixtures (GPM-SS) were numbered from 1 to 6 for each type of powders mixtures as pressure increase from 100 to 600 MPa.

The tribological tests for determining the friction coefficient and wear rate were performed at room temperature with a ball-on-disk standard tribometer (CSM Instruments) equipped with a rotating module. A 100 Cr6 steel ball bearing of 6 mm in diameter was used as the static contact partner.

The specimens were placed in the tribometer rotating module at different sliding radius (R) of 2 mm, 4 mm or 6 mm and the elastic arm of the tribometer was loaded with a fixed normal load (Fn) of 1 N, 2 N or 5 N. Sliding distance was preset at 20 m and linear speed was 3.5 cm/s. Data acquisition frequency was 20 Hz. The deflection of the static partner was measured for load and it was recorded as a tangential force (Ft). Sliding friction coefficient (μ) was calculated as the ratio of Ft to Fn with the equation (1) [14]:

$$\mu = \frac{F_t}{F_n} \qquad (1)$$

The wear rate (in mm^3/Nm) of the specimens was calculated by measuring the volume of the material removed and normalizing that to the load (Fn, in N) and the distance (L, in m) travelled during the test by the equation (2) [13]:

$$wear\ rate = \frac{V}{LF_n}\ [mm^3/Nm] \qquad (2)$$

To measure the volume of track material removed, track profiles were taken after testing using a Surtronic 25 stylus profilometer (Taylor Hobson) with Gaussian filter on an evaluation length of 4 mm, Cut-off of 0.8 mm and traverse speed of 1 mm/s.

Composite surface and fracture of the specimens were investigated by scanning electron microscopy (SEM) with an Auriga Zeiss microscope. Further are presented the results only for the sample 1 of non-granulated powders mixtures specimens (NGPM-S) and sample 1 of granulated powders mixtures specimens (GPM-S) type.

3. Results and discussions

3.1 Tribological results

In Table 1 and Table 2 are shown the tribological properties of NGPM-S and GPM-S. The friction coefficient varied from 0.180 to 0.784 for the sintered specimens made of NGPM-S and from 0.212 to 0.813 for the sintered specimens made of GPM-S.

The friction coefficient values of both NGPM-S and GPM-S materials decrease with the increase of the loading force.

The wear rate varied from 4.245×10^{-4} to 235.6×10^{-4} mm^3/Nm for NGPM-S specimens and from 6.049×10^{-4} to 254.7×10^{-4} mm^3/Nm for GPM-S specimens.

The majority of GPM-S specimens show higher wear rate values than the NGPM-S specimens suggesting the fact that the granulation operation is contraindicated for this kind of materials.

Table 1.Tribological properties of NGPM-S specimens

Sample No.	*NGPM-SS*					
	Average friction coefficient Fn [N]			*Wear rate [mm^3/Nm] Fn [N]*		
	1	2	5	1	2	5
1	0.187	0.197	0.180	4.577×10^{-4}	4.622×10^{-4}	4.245×10^{-4}
2	0.208	0.459	0.618	4.385×10^{-4}	34.10×10^{-4}	127.4×10^{-4}
3	0.241	0.578	0.784	168.1×10^{-4}	235.6×10^{-4}	132.4×10^{-4}
4	0.310	0.574	0.730	30.46×10^{-4}	88.82×10^{-4}	170.6×10^{-4}
5	0.321	0.452	0.465	37.44×10^{-4}	29.22×10^{-4}	27.18×10^{-4}
6	0.333	0.363	0.597	106.3×10^{-4}	136.0×10^{-4}	47.74×10^{-4}

Table 2.Tribological properties of GPM-S specimens

Sample No.	*GPM-SS*					
	Average friction coefficient Fn [N]			*Wear rate [mm^3/Nm] Fn [N]*		
	1	2	5	1	2	5
1	0.249	0.238	0.233	6.049 x 10^{-4}	7.795 x 10^{-4}	12.32 x 10^{-4}
2	0.212	0.223	0.473	44.39 x 10^{-4}	166.2 x 10^{-4}	254.7 x 10^{-4}
3	0.471	0.578	0.639	20.73 x 10^{-4}	62.92 x 10^{-4}	111 x 10^{-4}
4	0.417	0.689	0.813	170.4 x 10^{-4}	110 x 10^{-4}	162.5 x 10^{-4}
5	0.428	0.568	0.758	19.36 x10^{-4}	138.1 x 10^{-4}	166.4 x 10^{-4}
6	0.415	0.652	0.802	74.21 x 10^{-4}	156.4 x 10^{-4}	153.2 x 10^{-4}

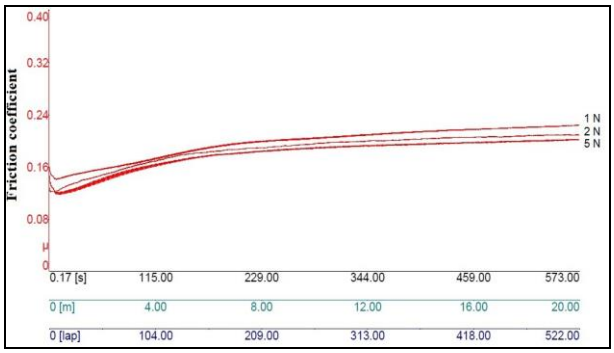

(a)

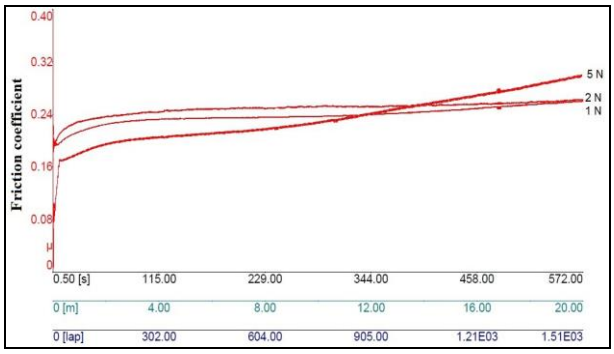

(b)

Fig. 1. Friction coefficient comparison over the time, total distance and laps, respectively for the specimen 1 of (a) NGPM-S and (b) GPM-S material type.

In Fig. 1 can be observed that the friction coefficient of the both NGPM-S and GPM-S materials reached a steady state where the surfaces of the static partner (steel ball) and specimen are running smoothly over each other, after the sliding distance of 6 m and 2 m respectively for the NGPM-S material (steady state friction of 0.18-0.19) and GPM-S one respectively (steady state friction of 0.23-0.24). The powders granulation led to an increase of the friction coefficient values which justifies the wear rate increase for the GPM-S specimens. All the tested samples exhibited wear tracks visible with naked eye having an increase depth with increase of loads. The best tribological behavior exhibited both NGPM-S and GPM-S specimens pressed at the lowest pressure, namely 100 MPa. Friction coefficient comparison over the time, total distance and laps, respectively for the specimen 1 of NGPM-SS and GPM-S types are presented in Fig. 1 (a) and (b).

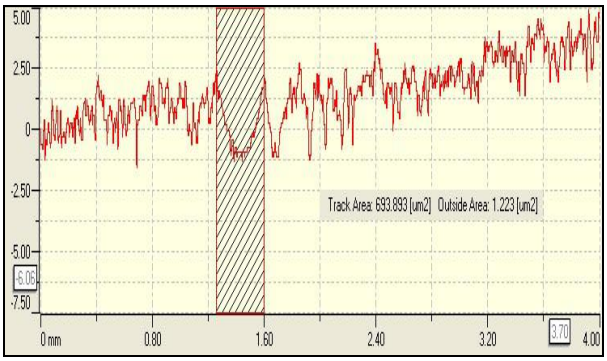

(a)

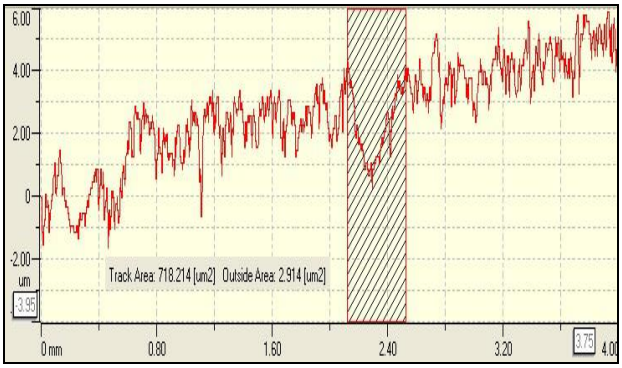

(b)

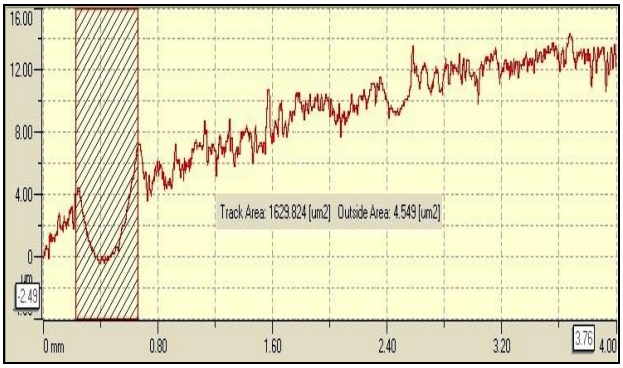

(c)

Fig. 2. Images of wear track profiles versus evaluation length for the specimen 1 of NGPM-S type tested at a load and radius of: (a) 1 N and 2 mm, (b) 2 N and 4 mm, (c) 5 N and 6 mm.

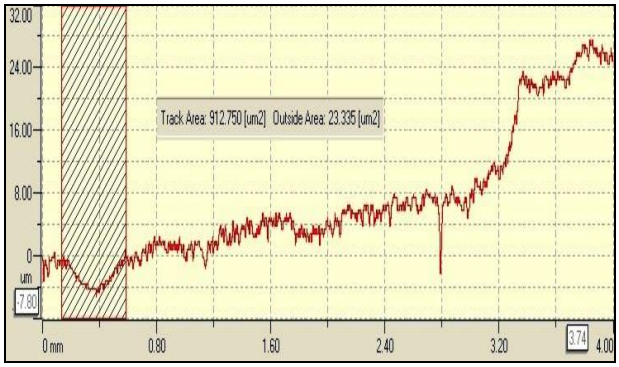

(a)

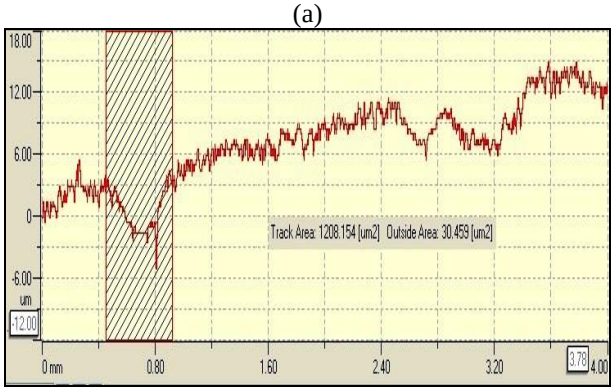

(b)

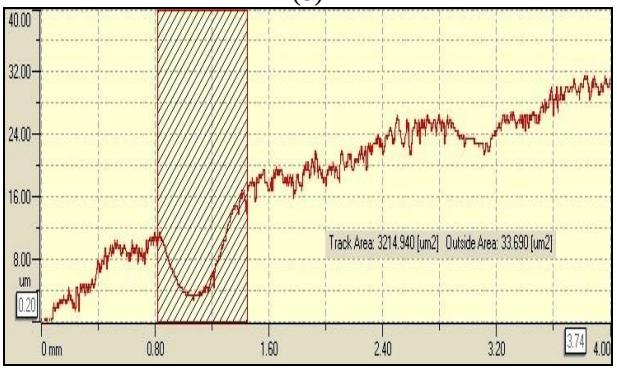

(c)

Fig. 3. Images of wear track profiles versus evaluation length for the specimen 1 of GPM-S type tested at a load and radius of: (a) 1 N and 2 mm, ((b) 2 N and 4 mm, (c) 5 N and 6 mm

The NGPM-S material exhibited a higher running-in period than the GPM-S material when the surfaces of the static partner and specimen are becoming bedded to each other. The fact that the friction coefficient is stable indicates a sintered material with a good mechanical embedding of Al_2O_3 and Gr particles in the Al metal matrix.

Figs. 2 and 3 show images of wear track profiles versus evaluation length for the specimen 1 of NGPM-S and NGPM-S material type tested at different conditions

3.2 Microstructure

SEM images for the specimen 1 of GPM-S material type at different magnifications are presented in Fig. 4. Fig. 4 (a) and (b) show the aspect of the sintered material microstructure.

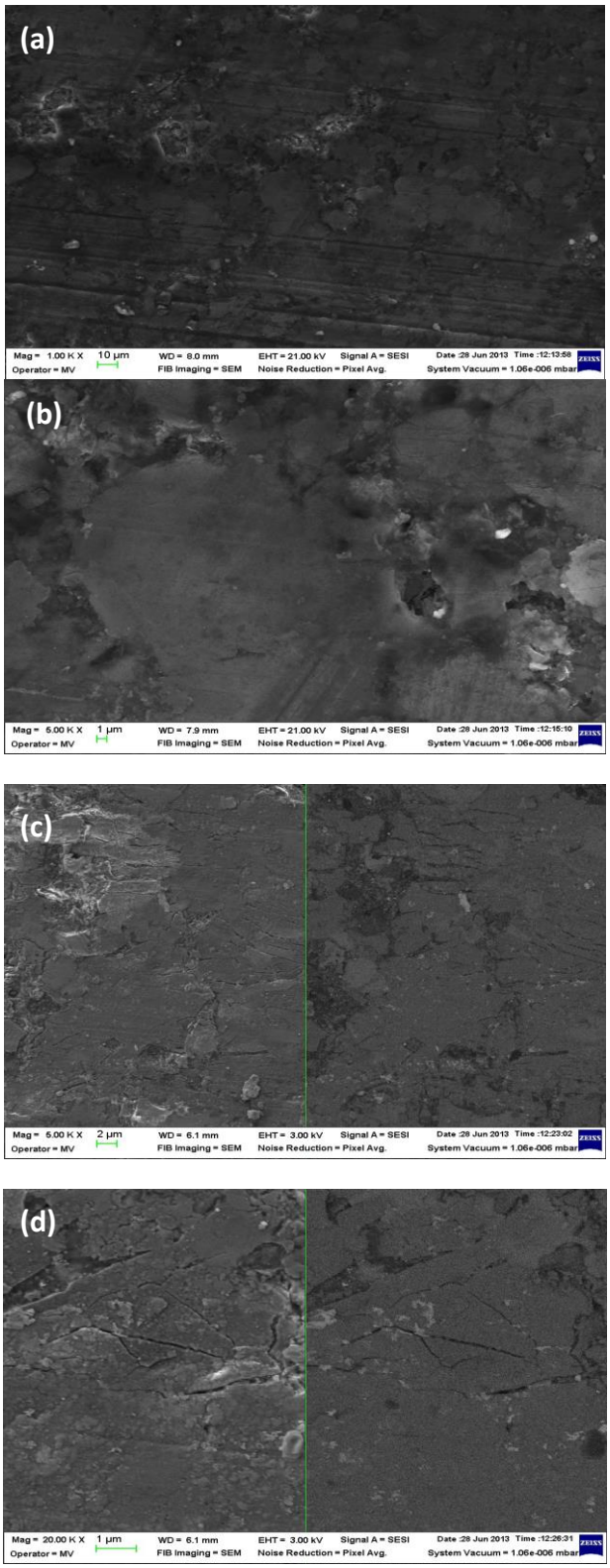

Fig. 4. Al/Al_2O_3/Gr hybrid composite SEM microscopy secondary and backscattered electron combined surface images: (a) SEM image magnified at 10 µm; (b) SEM image magnified at1 µm; (c) SEM image magnified at 2 µm; (d) SEM image magnified 1 µm.

We can distinguish a well sintered Al metal matrix where Al_2O_3 strengthening particles and Gr lubricant particles are strong embedded in the matrix, around 1-2

μm are identified. In Fig. 4 (c) are presented combined secondary electrons and backscattered electrons images which reveal topography and morphology of the surface but also the composition of the material. A magnification of the red marked area shown in Fig.4 (d) reveals the sintered Al metal matrix and the reinforcing particles distributed in the aluminum matrix.

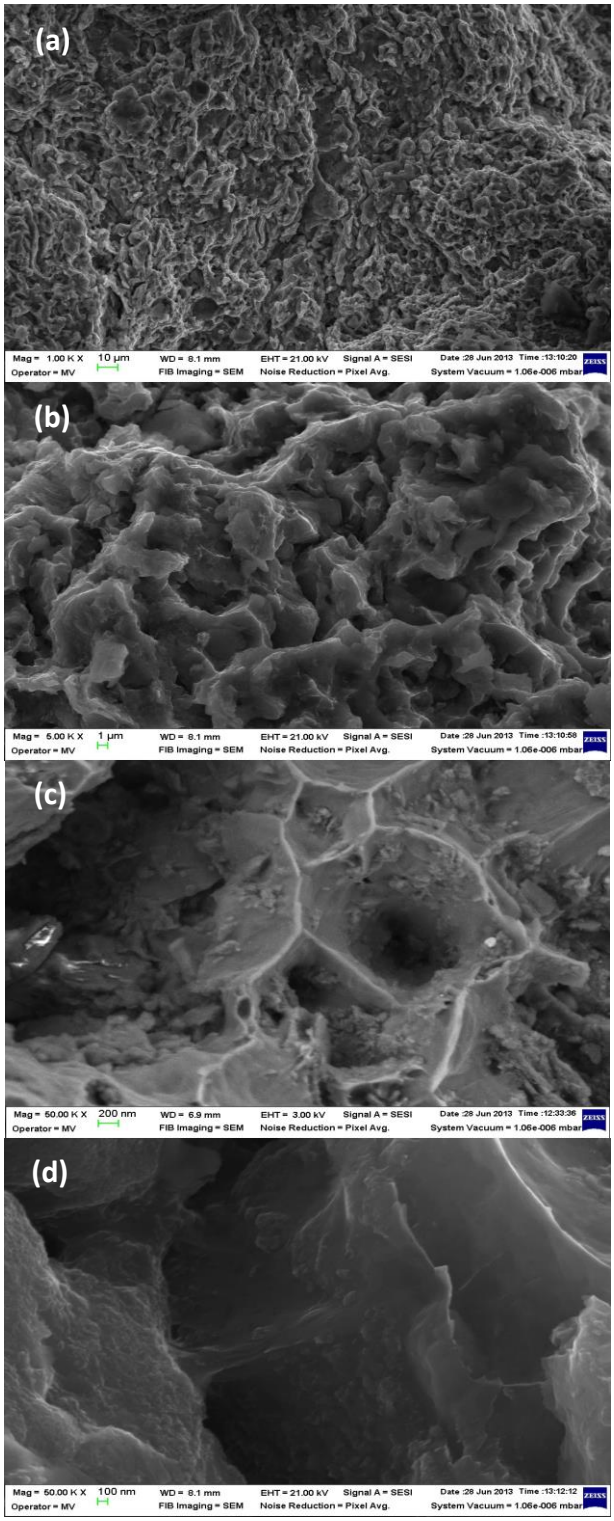

Fig. 5. Al/Al_2O_3/Gr hybrid composite SEM images of fractured area at different magnifications. (a) 10 μm; (b) 1 μm; (c) 200 nm; (d) 100 nm.

There are also some areas with Al_2O_3 clusters, which in some places may be the reason for hindering the sintering process. Also the presence of some micro and macro pores with dimensions around 1-2 μm are identified.

Fracture surface for the specimen 1 of GPM-S material type was also examined through SEM microscopy (Fig. 5). Fig.5 (a) and (b) reveal the ductile – brittle fracture appearance. By magnifying the area, in Figs. 5 (c) and (d), it can be seen that the fracture of the material occurred on the Al_2O_3 cluster zone, precisely at the grains boundaries, meaning that the areas with Al_2O_3 agglomerations provides fragility to the material.

4. Conclusions

Tribological and microstructure properties of Al/Al_2O_3/Gr hybrid composite containing an aluminum matrix reinforced with 4.5 wt.% alumina (Al_2O_3) and 0.5 wt.% graphite (Gr) particles fabricated through powder metallurgy route were investigated.

Sintered specimens exhibited an average friction coefficient of 0.180 to 0.784 for the ones made of non-granulated powders mixtures (NGPM-S) and from 0.212 to 0.813 for the ones made of granulated powders mixtures (GPM-S).

The wear rate varied from 4.245 x 10^{-4} to 235.6 x 10^{-4} mm3/Nm for NGPM-S specimens and from 6.049 x 10^{-4} to 254.7 x 10^{-4} mm3/Nm for GPM-S specimens.

Sintered specimens obtained from both non-granulated and granulated powder pressed at 100 MPa had the best sliding properties especially for the NGPM-S material type.

SEM microstructure reveals a good Al metal matrix sintering and the homogenous dispersion of reinforcement particles in the matrix with the fracture occurred at the Al_2O_3 particle boundaries.

The results were influenced by the processing of the powders mixtures, the compacting pressure applied to obtain green compacts, the homogeneity of the obtained microstructure after sintering process and the tribological testing conditions.

Acknowledgments

The work has been funded by the Sectorial Operational Programme Human Resources Development 2007-2013 of the Ministry of European Funds through the Financial Agreement POSDRU/159/1.5/S/132395.

References

[1] M. K. Surappa, Aluminum matrix composites: Challenges and Opportunities. Sadhana. **28**, Parts 1 & 2, 319 (2003).

[2] J. M. Mendoza-Duarte et al., J. Alloys Comp. http://dx.doi.org/10.1016/j.jallcom.2015.01.018 (2015).

[3] M. Kumar, A. Megalingam, V. Baskaran. Dry Sliding Tribological Characterization and Parameters Optimization of Aluminum Hybrid Metal Matrix Composite for Automobile Brake Rotor Applications. International Conference on Advances in Design and Manufacturing (ICAD&M'14), p. 368 – 373. (2014).
[4] T. Rajmohan, K. Palanikumar, S. Ranganathan. Trans. Nonferrous Met. Soc. China **23**, 2509 (2013).
[5] S.V. Prasad, R. Asthana. Aluminum Metal–Matrix Tribology Letters, **17(**3), (2004).
[6] G. B. Veeresh Kumar1, C. S. P. Rao, N. Selvaraj. Journal of Minerals & Materials Characterization & Engineering, **10**(1), 59 (2011).
[7] M. Kök, K. Özdin. Journal of Materials Processing Technology **183**, 301 (2007).
[8] N. Radhika, R. Subramanian, S. Venkat Prasat. Journal of Minerals & Materials Characterization & Engineering, **10**(5), 427 (2011).
[9] Vencl, A. Rac, I. Bobić. Tribological Behaviour of Al-Based MMCs and Their Application in Automotive Industry. Tribology in industry, **26**(3&4), 31 (2004).
[10] R. Deaquino-Lara, N. Soltani, A. Bahrami, E. Gutiérrez-Castañed, E. García-Sánchez, M. A. L. Hernandez-Rodríguez, Materials and Design **67**, 224 (2015).
[11] P. Ravindrana, K. Manisekar, R. Narayanasamy, P. Narayanasamy, Ceramics International **39**, 1169 (2013).
[12] Ana Veteleanu, Metalurgia International, **XVII** (4), 122 (2012).
[13] A. Baradeswaran, Elaya Perumal. Composites: Part B **56**, 464 (2014).
[14] D. A. Smith, T-09-113-Wear and Friction Analysis of Thin Coatings, Silcotek Tribology Testing Report, (2009).

* Corresponding author: ioana.apostolescu@upb.ro